## PASSIVELY ACTUATED, TRIANGULAR RADIATOR FIN ARRAY

Josh R. Cannon, Brian D. Iverson Brigham Young University, Provo UT 84604

Wenbin Song, Rydge B. Mulford University of Dayton, Dayton OH, 45469

### **ABSTRACT**

Thermal control is a challenge for spacecraft as they must maintain internal components within operating limits despite significant fluctuations in external and internal thermal loads. Satellites often rely on dynamic thermal control to manage internal temperatures depending on the thermal environment. However, many of these systems are actively managed, relying on the satellite's internal electronics to control the radiator's behavior. The problem of thermal control is compounded for small satellites, such as CubeSats, which have high power dissipation per unit surface area, stringent size/weight restrictions, and reduced thermal mass. Passive thermal control is particularly attractive for such small systems, potentially offering increased reliability and simplicity. Attempts at passive, dynamic thermal control of spacecraft radiators have been demonstrated in the literature using louvers actuated by bimetallic coils and radiators deployed by shape memory alloys. In this work, we propose a dynamic thermal control method for CubeSats by using bimetallic coils to passively deploy an array of four triangular radiator fins that, when folded, comprise the external face of a CubeSat. This approach differs from previous approaches as it uses mass efficient, triangular radiative fins as well as bimetallic coils to passively actuate the panels, as opposed to shape memory alloys. The advantages of this design include reduced complexity, cost, volume, and weight when compared to traditional deployable radiators in addition to increased redundancy by using an array of panels. An experimental demonstration of the proposed design is presented indicating the ability to passively deploy a single radiator fin using custom bimetallic coils at a rate of approximately 3.9° of angular rotation per 1 °C with minimal hysteresis. A preliminary model of our design indicates the possibility to achieve a turndown ratio of greater than 7:1. Experimental and numerical prediction results are presented as a motivation for exploration of the proposed design in ongoing work.

### 1 INTRODUCTION

## 1.1 CubeSat Thermal Design

As the miniaturization of control electronics and instruments improves, small satellites such as CubeSats are being used for an increasing variety of payloads and in more diverse mission locations. CubeSat developers must employ novel solutions for thermal control of their spacecraft with this increasing system complexity and function. Small satellite thermal control can be challenging due to:

- Large fluctuation in external heat input While orbiting the Earth, a spacecraft experiences significant variation in external heat flux. In the extreme external heating case, a satellite receives direct solar heating, as well as albedo and infrared radiation from the Earth. Alternatively, the extreme cold case occurs when the satellite is positioned in the umbra of the earth without direct solar heating or albedo radiation. For satellites orbiting the Moon, the fluctuation can be even more pronounced due to the presence or absence of albedo and infrared radiation from the moon and Earth.
- Large fluctuation in internal heat load Many satellite missions use instruments that may be turned on periodically, generating large amounts of waste heat. Use of these instruments may not be synchronous with the external heating cold case during orbit.
- Small form factor CubeSats can suffer from high power dissipation per unit surface area,
  more stringent size/weight restrictions, and reduced thermal mass when compared to
  larger spacecraft. Small satellites such as CubeSats have added challenges due to the
  requirements of the CubeSat Form Factor, which controls the external geometry of the
  satellite and limits the thermal mass present in the spacecraft.

Despite these challenges, a satellite's components may be required to operate within a specified temperature range. To achieve this, CubeSat developers typically use either static or dynamic thermal control. We define static thermal control systems as those systems that employ radiators which maintain a constant geometry and radiative properties. As such, heat rejection varies only according to the internal temperature of the satellite. Although simple, this methodology typically requires that the satellite's radiator be sized to accommodate the maximum required heat loss at all times (cold-biasing). However, this strategy may result in excessive heat rejection during the coldest parts of the orbit and utilization of onboard heaters to increase the temperature.<sup>1</sup> Such heating can negatively affect size, weight and power requirements. Regardless, an advantage of static radiators is their simplicity.

Dynamic thermal control systems, on the other hand, utilize passive or active variations in the radiator's surface properties or geometry to vary the heat rejection rate according to need. This allows a satellite to reject sufficient heat during the hot case to avoid significantly increasing the onboard temperature. Dynamic thermal control can allow satellites to perform a greater variety of mission functions in more challenging thermal environments (such as lunar orbit) but at the cost of increased complexity and, potentially, increased size and weight requirements. The versatility of dynamic thermal management makes it attractive for small satellite developers.

## 1.2 <u>Dynamic Thermal Control</u>

Dynamic radiator technologies often modify either the surface properties of the radiator, the surface geometry, or both to adapt to variable heat loads. Examples include thermochromics<sup>2</sup> and electrochromics<sup>3</sup> which modulate the emissivity of the radiator. Another broad category is deployable radiators, which includes conceal and reveal radiators that typically have a low emissivity coating on the outside and deploy to reveal a higher emissivity coating on the interior<sup>4</sup> or provide a direct radiative path to the interior of a satellite (e.g. louvers<sup>5</sup>). Other deployable

radiators expand and contract primarily to alter the effective surface area (e.g. accordion radiators<sup>6</sup>).

In addition to offering a potentially high turndown ratio, deployable radiators also can reject the greatest amount of heat among common state-of-the-art radiator designs. A high turndown ratio makes a deployable radiator more suitable for missions that have widely fluctuating thermal environments. However, deployable radiators can have the drawback of increasing component complexity. Additionally, reliability can be a concern, since deployable radiators are likely to be controlled electronically by the onboard control system. If the control system fails, a CubeSat's temperature may quickly exceed the desired operating temperature limits.

# 1.3 Passively Deployed Radiators

Passively deployed radiators offer the potential of dynamic thermal control without the added system complexity and control system dependence. Thermally driven, passive actuators capable of deploying a small satellite radiator exist, including Shape Memory Alloys (SMAs), and bimetallic coils.

SMA's rely on a temperature-driven, solid-solid phase transformation to produce a one-way "shape memory" effect. This means an SMA can be trained so that when heated, it will return to its original shape, regardless of any deformation the material has subsequently undergone. 8 One SMA actuator design involves training a length of SMA wire into a spring shape. A bias spring is then used to apply a constant torque to the SMA, causing it to deflect. When the SMA temperature increases, the solid-solid phase transformation increases the torque applied by the SMA, allowing it to overcome the bias spring and return to its previous, undeflected shape. As the SMA spring begins to cool, the state transition is reversed and the bias spring's torque becomes dominant again, deflecting the SMA. SMA actuators have the advantage of being small and light relative to the force they can produce. However, once SMA actuators reach their transition temperature, the actuation occurs relatively rapidly, resulting in bi-modal operation with a deployable radiator panel being positioned in an either fully open or closed configuration (rather than being able to reach steady state in a partially open configuration). Additionally, SMA actuators can experience hysteresis of 10 °C between deployment and retraction. 10 Nagano, et al. have developed a single deployable radiator which is actuated by an SMA element. As the temperature of the satellite increases, a strip of SMA is designed to unfold, deploying the panel and revealing a highly emissive surface. Through on-the-ground testing, they have demonstrated that the SMA actuator can deploy and stow the panel as the SMA temperatures cycle between ±30 °C.<sup>11</sup>

Bimetallic coils are comprised of two sheets of metals with different coefficients of thermal expansion bonded together. As the coil heats up, the metals expand at different rates, causing a coil to curl or uncurl, depending on the configuration. When the coil cools, it relaxes and returns to the undeflected state. Because bimetallic coil actuators are less energy dense than SMA actuators, they are typically heavier and larger. This increased size can slow the heat transfer to the actuator, causing the panel deployment to respond more sluggishly. One advantage of

bimetallic actuators is that there is a linear relationship between the temperature of the coil and the angle of deployment of the radiator. The radiator is able to maintain intermediate geometric positions at steady state conditions, unlike SMA actuators. Bimetallic coils have been successfully demonstrated on orbit as passive actuators for thermal louvers in the Dellingr CubeSat in 2018.<sup>12</sup>

In this work, an initial prototype for a passively actuated dynamic radiator is described and preliminary tests are run to establish the validity of the approach and lay the ground for more robust testing and design. To improve reliability and reduce complexity while still achieving a high turndown ratio with deployable radiators, we propose a dynamic, passively deployed radiator fin array consisting of triangular panels. The triangular panels are actuated with bimetallic coils that deploy in response to an increase in CubeSat temperature. This approach is novel as it is the first CubeSat thermal control system that employs an array of passively deployable panels for increased redundancy and efficiency, in addition to being the first to use bimetallic coils to passively actuate a radiator panel. A prototype is experimentally tested in a vacuum chamber to demonstrate deployment and to determine the relationship between deployment angle and temperature. A thermal model is used to predict heat loss from a CubeSat face with 4 deployable triangular radiator panels. The experimentally verified dynamic actuation of the radiator is then described and the thermal model results are presented to explore the possible range of turndown ratio.

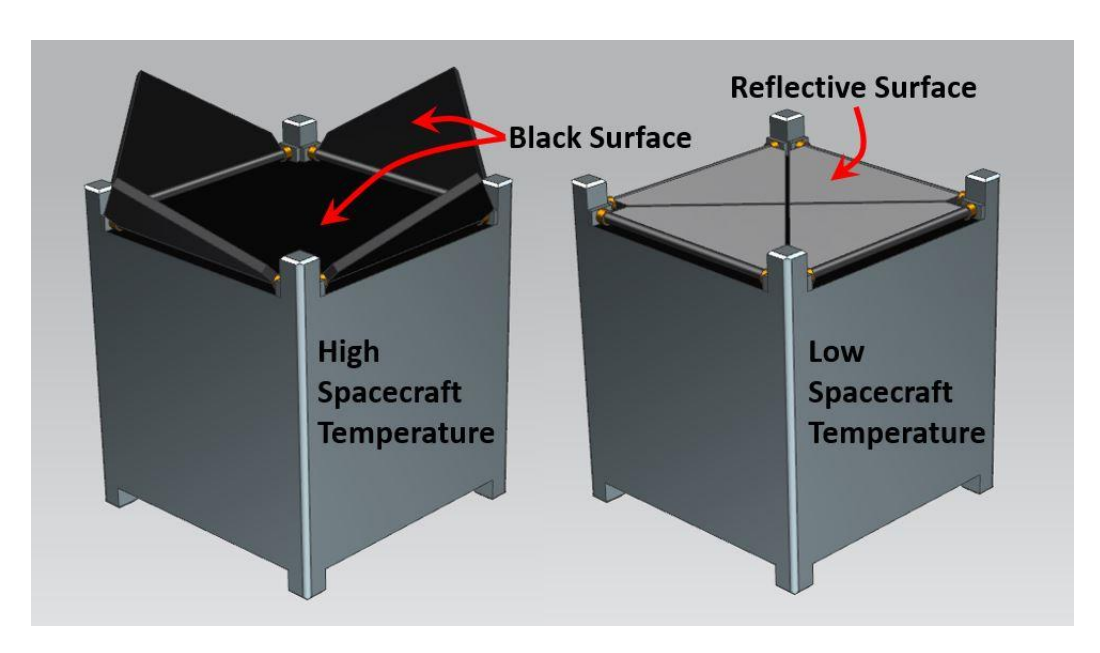


Figure 1. Illustration of deployed and stowed radiator panels for CubeSat thermal management.

### 2 METHODS

### 2.1 Prototype

The dynamic radiator consists of four triangular fins that are actuated independently by bimetallic coils as illustrated in Figure 1. Although SMA's can produce a larger actuation torque

than the bimetallic coil given equivalent sizes, some of this advantage is lessened by the fact that SMAs require a bias spring while bimetallic coils do not. Further, the use of bimetallic coils as the method of actuation allows the angle of radiator deployment to vary continuously (with a linear relationship), as driven by the internal temperature of the satellite. This is in contrast to alternative actuation methods with binary states, such as shape memory alloys. Triangular, rather than rectangular, radiator panels are utilized to improve fin efficiency and the ratio of heat rejection to component mass. With four panels operating in parallel, there is added redundancy in the thermal control system compared to state-of-the-art passively deployable radiators, such as those developed by Nagano et al., <sup>11</sup> which actuate one or two panels.

Each of the radiator panels is attached to a conductive rod/hinge with a bimetallic coil at each end. One end of each coil is attached to the CubeSat's frame, while the other is attached to the rod. As the temperature of the coils increases, they curl and rotate the rod, deploying the radiator panel to an open position. In this open position, the heat loss from the panel is increased, reducing the temperature of the CubeSat. Heat is transferred from the rod and satellite frame to the coil through conduction, as well as through radiation from the CubeSat interior to the panel. To increase the turndown ratio of future prototypes, internal surfaces of the radiator panels will be coated with a high emissivity paint while the exterior faces will be reflective.

The completed, single-panel test article can be seen in Figure 2c. The radiator panel, conductive rod, brackets holding the rod, and CubeSat frame stand-in were all manufactured from aluminum stock. The custom bimetallic coils were manufactured by Crest Manufacturing out of P675R due to its high flexitivity. The springs are 15 mm in overall diameter consisting of bimetallic strips measuring 6.4 mm wide by 0.18 mm thick. Stainless-steel, ball-bearing washers were added to the ends of the rod to reduce friction during rotation.

The CubeSat frame stand-in was sized to be half of a standard CubeSat face (100 mm x 50 mm) and is 4.8 mm thick. The triangular fin was sized so that 4 fins would cover a single CubeSat face, leaving enough room for actuation; each fin has a width of 73 mm, a height of 43 mm, and a thickness of 1.5 mm. The tips of the two base corners were removed to accommodate the bimetallic coils.

# 2.2 <u>Experimental Demonstration</u>

The goal of the experiment was to demonstrate a dynamic response of a radiator to an increase in operating temperature by actuating fin position using bimetallic coils as a linear function of temperature. The test system shown in Figure 2a includes a vacuum chamber, data acquisition system, rotary motion sensor, power supply, test article, thin-film heater, thermocouples, and fixturing. The test article was fixed to an optical plate and contact points between the CubeSat frame and test fixtures were insulated with 3.2 mm thick plates of G10. The test article was then placed in a cylindrical vacuum chamber 70 cm wide and 76.2 cm long. The CubeSat frame was heated by a thin film Kapton heater connected to a power supply via vacuum chamber feedthroughs. Seven T-type thermocouples were epoxied onto the test article at positions indicated in Figure 2b. The thermocouple cables were connected to a LabView data acquisition

system through additional feedthroughs. Rotation of the triangular radiator panel was measured by a Vernier Rotatory Motion Sensor connected to the axis of rotation of the rod which had a resolution of 0.25°.

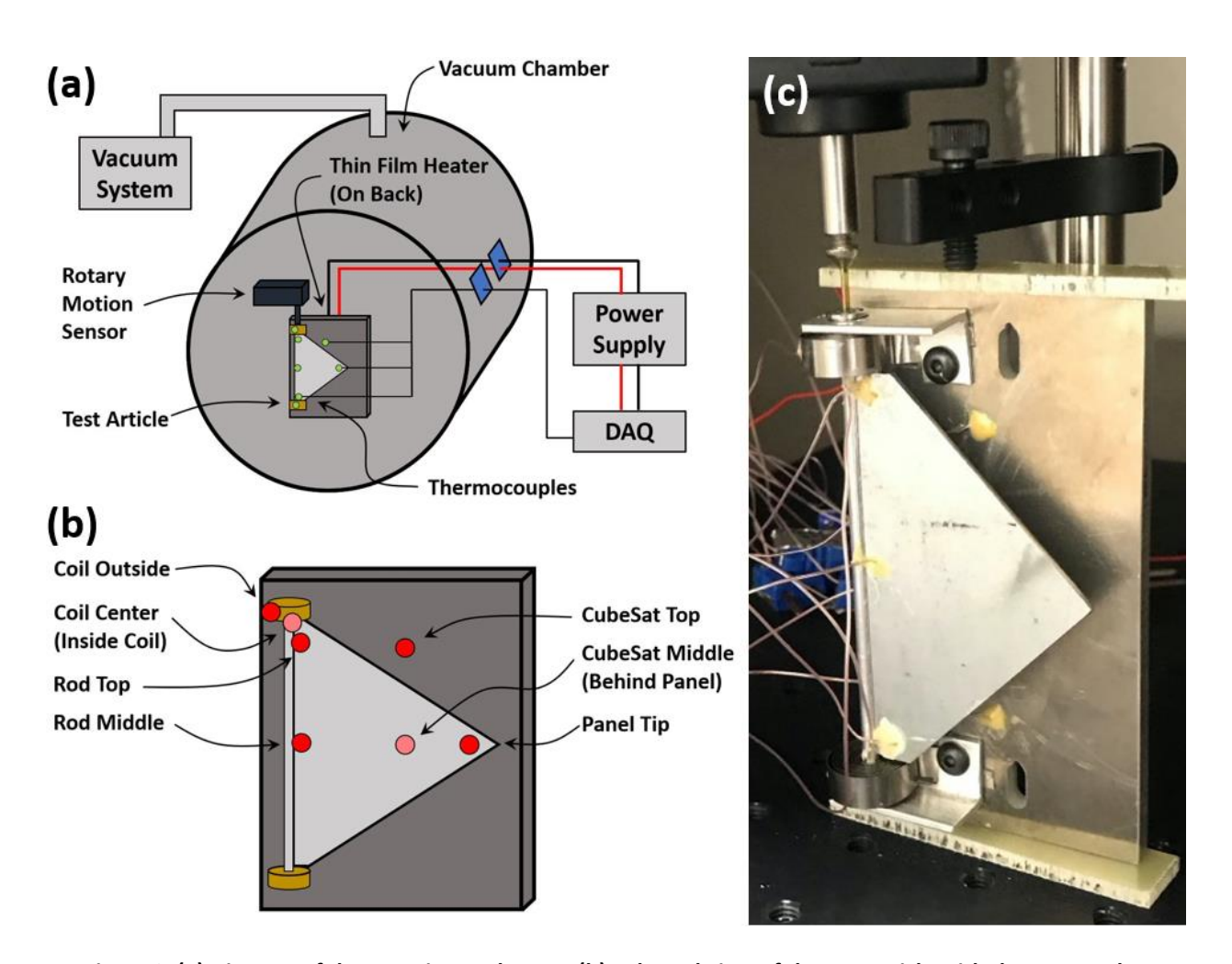


Figure 2. (a) Diagram of the experimental setup. (b) Enlarged view of the test article with thermocouple locations labeled. (c) Test article mounted in the vacuum chamber with the rotary motion sensor.

Once the vacuum chamber was pumped down to a pressure less than 2x10<sup>-5</sup> torr, (sufficient to ensure that losses due to convection were negligible, <sup>13</sup>) the power supply was turned on and the temperature setpoint was selected. As the purpose of this research was to establish a relationship between the temperature of the bimetallic coil and the angle of rotation of the panel, and thus provide an initial demonstration of the validity of our design, we elected to simulate an operating temperature range of 0-85 °C. Since the ambient temperature was 20 °C, this meant that the temperature setpoint for the tests was 105 °C. While such a large temperature range may be larger than what is allowable for some satellites, this range enabled exploration of the approach and the extent of performance of the coils. Using two

thermocouples attached to the CubeSat frame as reference, a PID temperature controller cycled the power supply on and off in order to maintain the frame at the setpoint temperature. 14

The CubeSat frame was maintained at 105 °C until steady state was reached (considered to be when the average rod temperature changed by less than 1 °C over the course of 10 min) and then held there for another 45 min. The power supply was then shut off and the test article was allowed to cool.

# 2.3 Thermal Model

The heat transfer relative to the radiator deployment angle for a set of 4 triangular radiator panels was modeled using a computational heat transfer package in Solidworks. The purpose of the model is to determine the potential turndown ratio that a CubeSat thermal control system using four triangular radiator fins could achieve. Thus, the steady state model assumes the main CubeSat body and fins are aluminum and have a thermal conductivity of 170 W m<sup>-1</sup> K<sup>-1</sup> and a thermal resistance of 0.01 K W<sup>-1</sup> between the CubeSat body and an individual triangular fin. This thermal resistance is typical for a heat pipe,<sup>15</sup> which is one method in which the radiator panels and the CubeSat body could be thermally connected in a finalized design. Currently, the test article described above conducts heat from the CubeSat

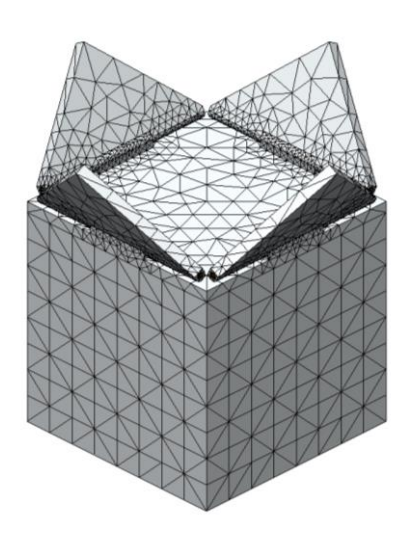


Figure 3. FEA mesh in SolidWorks.

face to the radiator panel primarily via conduction through the ball bearing washers the rod is mounted to and thus has a much higher thermal resistance. The model also omits the behavior of the bimetallic coils and their transient response to changes in temperature. Instead, the panels are rotated manually and the change in radiative heat loss is observed.

The outer surfaces of the triangular fins (exposed to space when the fin is stowed) have an emissivity of 0.1, whereas the interior surfaces of the fins and the top of the CubeSat (exposed to space when the fins are fully deployed) have an emissivity of 0.9. Results are calculated for a constant CubeSat temperature of 273 K and a deep space temperature of 4 K. The CubeSat temperature of 273 K was selected because it is on the low end of the temperature ranges generally targeted by CubeSats and thus produces a more conservative estimate for maximum turndown ratio.

Tetrahedral elements in a curvature-based mesh (Figure 3) were used with a global element size of 2.59 mm. Near the base of the fin, a finer mesh was applied to increase the accuracy of the simulation. The heat loss was then computed as the angle of the panels was varied from 0° to 180° (relative to the closed position).

#### 3 RESULTS

## 3.1 Experimental

Three separate prototype tests were performed. Figure 4a shows the temperature data collected from the seven thermocouples during a representative test and is separated into three stages: heating, steady state, and cooling as the power supply is turned off. The thermocouple locations used to collect the temperature data are shown in Figure 2b. The CubeSat Top and CubeSat Middle temperatures are used as the reference temperatures for the PID temperature controller and behave as expected, heating quickly, reaching the set point, then cooling when the power supply is turned off in the cooling portion. Of the remaining thermocouples, the Coil Center and Coil Outside thermocouples record the next highest temperature, showing that initially, heat is flowing through the coil, from the outside to the center, and then to the rod and radiator panel. Future work on the prototype will incorporate a thermal hinge to decrease the thermal resistance between the CubeSat body and the radiator panel. This improved conduction path should cause heat to conduct to the coil from both ends (the CubeSat body and the rod/radiator panel) instead of through the coil to the radiator. The two thermocouples on the rod recorded the next warmest temperature and the Panel Tip thermocouple was the coolest, as expected for a radiator fin. As mentioned above, the two thermocouples attached to the rod were averaged and used to determine when steady state began (defined here as when the temperature changed by less than 1 °C in 10 min.). In this manner, steady state was determined to occur at approximately 45 min.

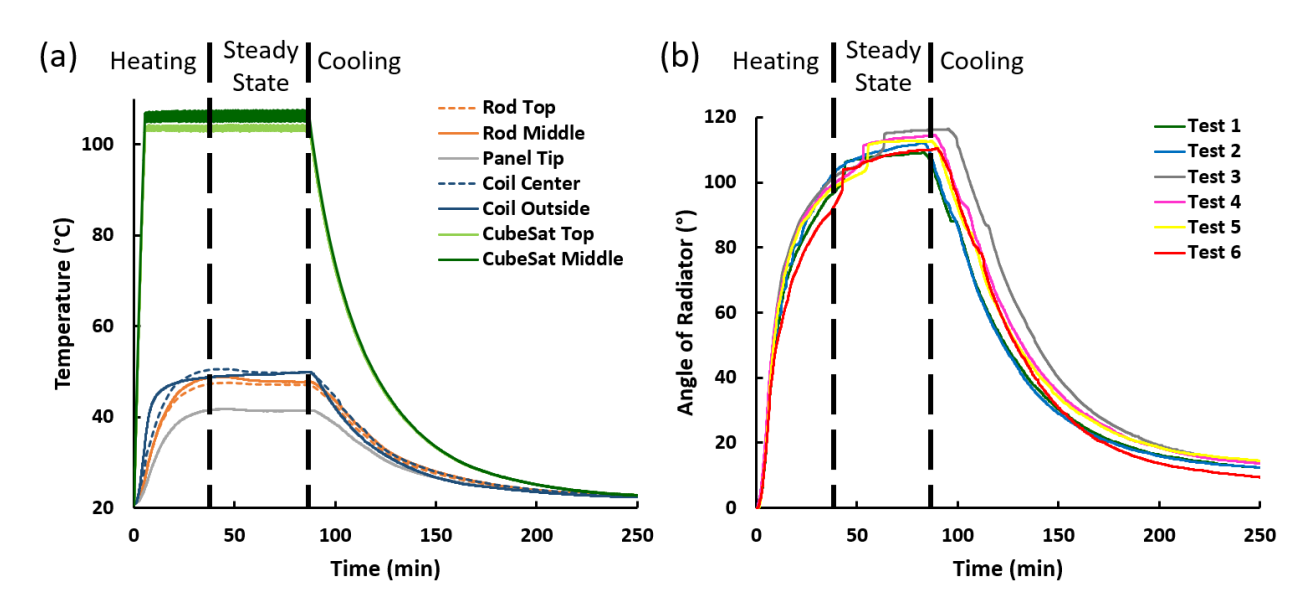


Figure 4. (a) Temperature as a function of time from thermocouples corresponding to the locations shown in Figure 2b. (b) Angle of the radiator panel as a function of time.

In Figure 4b, the radiator panel angle data as a function of time is presented for each of the tests. During the heating phase, the bimetallic coils rotate the panel predictably, however, during the steady state portion of the test, when the average temperature of the coil has leveled out (as measured by the thermocouples on the outside and in the center, the coils continue to rotate at

a slower rate. Additionally, some of the tests exhibited a sudden jump in the measured angle during the steady state portion. This is likely due to static friction in the system, especially at larger deployment angles; as the rotation rate slows this friction appears to prevent the coil from fully curling. The motion sensor may provide some resistance at higher deployment angles due to somewhat imprecise nature of its alignment with the rod, leading to the stickiness of the coils at those higher angles. It is assumed that further improving the alignment of the motion sensor, the ball bearing washer mounts, and the rod would reduce or eliminate the continued creep of the coil during stead state as well as the occasional jumps in deployment angle during that same period.

The average temperature of the bimetallic coil was then plotted as a function of the angle of the radiator panel at the same time. Two lines of best fit were calculated for the coil temperature vs. deployment angle plots for each test: one for the heating and steady state phases and the other for the cooling phase. The slopes for these lines of best fit and the associated R² values are given in Table 1. The magnitude of the slope represents the number of degrees of panel rotation per degree Celsius as the average coil temperature changes. The average slope during heating/steady state was found to be 3.85 ° rotation per 1 °C with an average R² value of 0.948. Likewise, the average slope for the cooling phase was 3.88 ° rotation per 1 °C with an average R² value of 0.991. It is noted that the two average slopes for heating and cooling over all the cycles of the test were close, but the average R² value for the cooling phase was much higher than for heating/steady state. This is likely due to increased friction in the system at higher deployment angles which, at slower rates of temperature change, causes the coils to not behave as linearly as in other portions of the test. It is thought that improving the alignment of the system, as mentioned above, will increase the R² value for the heating portion without changing the average slopes for the heating or cooling phases.

Table 1. Experimentally observed panel rotation per change in degrees Celsius with R-squared value obtained from a linear fit.

|             | Heating                    |                | Cooling                    |                |
|-------------|----------------------------|----------------|----------------------------|----------------|
| Test number | Slope<br>(° rotation / °C) | R <sup>2</sup> | Slope<br>(° rotation / °C) | R <sup>2</sup> |
| 1           | 3.71                       | 0.947          | 3.76                       | 0.993          |
| 2           | 4.00                       | 0.935          | 4.00                       | 0.990          |
| 3           | 3.85                       | 0.939          | 3.92                       | 0.989          |
| 4           | 4.03                       | 0.926          | 4.01                       | 0.992          |
| 5           | 3.69                       | 0.964          | 3.69                       | 0.993          |
| 6           | 3.15                       | 0.979          | 3.38                       | 0.991          |
| Average     | 3.85                       | 0.948          | 3.88                       | 0.991          |

## 3.2 Modeling

Figure 5 shows the results of the finite element analysis. As the angle of deployment of the triangular fins increases from 0° to 180°, radiative losses from both the top surface of the CubeSat body and the radiator panels increase. This is as expected since, as the panels deploy, more of the underlying CubeSat face (which is coated with a high emissivity paint) is exposed to space, increasing its ability to radiate. Similarly, the highly emissive undersides of the panels are exposed and pointing to space rather than at each other or the CubeSat. By dividing the modeled total radiative heat loss when the panels are fully open (180°) by the total heat loss when the panels are fully closed (0°), we calculate a turndown ratio of 7.65. At partial deployment, large turndown ratios are still possible. For instance, deployment from 0° to 90° results in a turn-down ratio of 4.7.

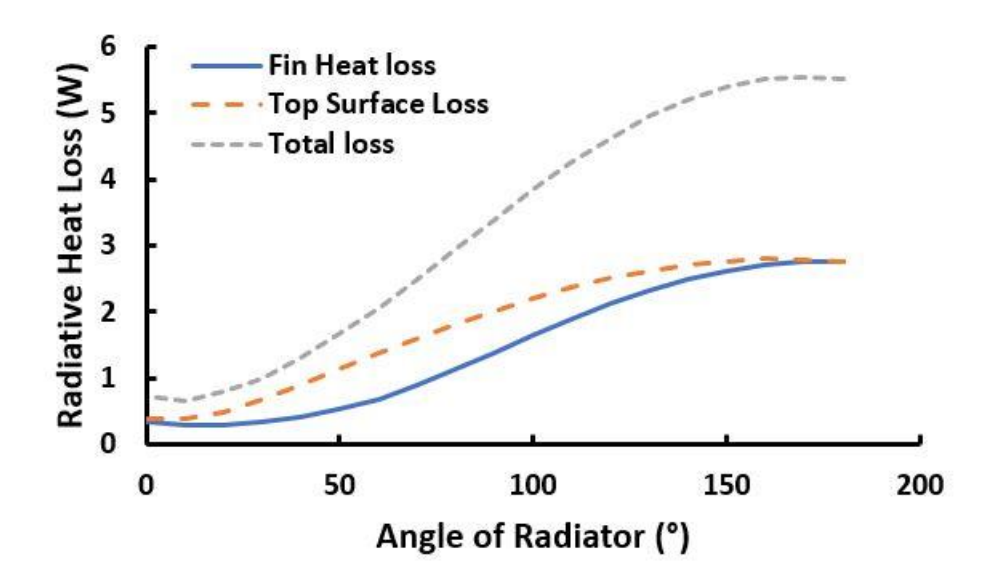


Figure 5. Modeled radiative heat loss from a 273 K CubeSat as a function of the radiator deployment angle.

### 4 DISCUSSION

The purpose of this research was to explore the viability of a dynamic thermal control system that relied on passively deployed radiator panels actuated by bimetallic coils. The experimental results presented in Table 1 suggest that there is a reliable, linear relationship between the temperature of the bimetallic coils and the angle of the deployable radiator panel. That is, for every degree Celsius the average coil temperature increases, we observed the panel to rotate approximately 3.85°, on average. Similarly, decreasing the coil temperature by 1 °C caused the panel to close by 3.88° degrees, on average. This means that in order to deploy the panels from 0° - 90°, the coils would need to be heated 23.4 °C (which, from the finite elements analysis described in this work suggests a turndown ratio of 4.7). In order to fully deploy the radiators from 0° - 180°, the coils would need to be heated 46.8 °C (for a predicted turndown ratio of 7.65). Passively achieving a turndown ratio of about 5 over a temperature change of 25 °C would be of value to many CubeSat missions. The finite element model of the four triangular radiator panels

demonstrated that as the panels are deployed, the radiative heat loss from the CubeSat increases. Together, these findings strengthen our confidence in the thermal control system described here and suggest that further exploration is warranted. However, several changes can be made to our experimental setup to improve the system and make it better reflect the thermal conditions it will experience onboard a CubeSat.

During the test cycles, when the CubeSat face was heated from 20 °C to 105 °C, the bimetallic coil and rod temperatures increased from 20 °C to 50 °C before reaching steady state. This suggests that there is significant heat loss through paths other than through the triangular radiator panel. It is expected that the conductive pathway between the frame of the CubeSat and the bimetallic coils/base of the radiator panel should be improved potentially by adding a thermal hinge, similar to that used by Nagano et al. <sup>11</sup> This would allow the bimetallic coils and the base of the triangular radiator to more closely track the temperature of the CubeSat frame. Given the same ratio between average coil temperature and angular rotation of the radiator panel, this would cause the panel to open up further for the same temperature increase in the CubeSat body. Put another way, the panels will deploy over 90° if the coil temperature increases by 25 °C; improving the conduction path from the CubeSat to the radiator panels and coils would mean the CubeSat temperature wouldn't need to vary as widely in order for the coils to increase those 25 °C and achieve the desired deployment. Thus, the radiator will be more responsive and narrow the temperature range experienced by the internal satellite components once a thermal hinge is added.

Additionally, for the experimental prototype to achieve the turndown ratios predicted in the FEA model, the interior surfaces of the radiator panel and the exterior surface of the CubeSat frame must be coated with a high emissivity paint and the exterior surface of the radiator with a low emissivity paint.

Finally, further work should be done on the thermal model to incorporate these findings on the relationship between the temperature of the coils and the rotation of the panels (which is that there is a linear relationship between the temperature of the coils and the deployment angle of the radiator of about 3.9 ° rotation per 1 °C). The improved model would include the transient response of the CubeSat and radiator systems, incorporating the temporal relationship between panel rotation and radiative heat loss. Additionally, the actual geometry of the system would be modeled with experimentally determined thermal conductivities and resistances. This model could then be verified experimentally in the vacuum chamber with an improved thermal measurement system such as an IR camera.

### 5 CONCLUSION

In this work, a novel triangular fin array passively actuated by bimetallic coils is proposed for use as a dynamic radiator. The advantages of this system include: 1) increased reliability due to the lack of electronic control and four panels operating in parallel, 2) high turndown ratio, 3) high maximum heat loss, 4) low weight and cost, 5) minimal hysteresis, and 6) continuous actuation

between fully closed and fully open states. An experimental demonstration finds that heating the face to which an experimental prototype is attached will cause the bimetallic coils to actuate and deploy a triangular aluminum fin at a rate of 3.85° rotation per °C with low hysteresis. A thermal model reveals that four triangular panels operating together achieve a turndown ratio of 7.65 when comparing the fully deployed and fully stowed cases. However, the current prototype demonstrates a large difference between the CubeSat temperature, and the temperature of the bimetallic coils and radiator. Further work is needed to provide a better conduction path (such as a thermal hinge) from the satellite body to the radiator to reduce this gap and allow the coils to be more responsive to changes in the CubeSat's internal temperature. In conclusion, the thermal management system described in this research offers specific advantages that warrant further investigation. The proposed approach is especially suited to small satellites in challenging thermal environments where accommodation of traditional active thermal control systems is not practical. Ongoing efforts include improving the thermal connection between the CubeSat interior temperature and the radiators/coils.

### **6 ACKNOWLEDGMENTS**

The authors acknowledge support provided by Vivek H. Dwivedi, NASA Goddard.

## 7 CONTACT

Emails of corresponding authors:

Rydge B. Mulford (rmulford1@udayton.edu), Brian D. Iverson (bdiverson@byu.edu)

## **REFERENCES**

- 1. Kang, S.-J., & Oh, H.-U. (2016). On-Orbit Thermal Design and Validation of 1 U Standardized CubeSat of STEP Cube Lab. *International Journal of Aerospace Engineering*, 2016, 4213189. https://doi.org/10.1155/2016/4213189
- 2. Kim, H., Cheung, K., Auyeung, R. C. Y., Wilson, D. E., Charipar, K. M., Piqué, A., & Charipar, N. A. (2019). VO2-based switchable radiator for spacecraft thermal control. *Scientific Reports*, *9*(1), 11329. https://doi.org/10.1038/s41598-019-47572-z
- 3. Kluge, O., Abendroth, B., Kohler, T., Altenburg, M., Borchardt, L., Abbe, E., Schuler, T., Zwiebler, A., Tajmar, M., & Schmiel, T. (2018). Electrochromics for Thermal Control on Spacecraft. *Proceedings of the 3rd World Congress on Momentum, Heat and Mass Transfer*, *2*, 1–8. <a href="https://doi.org/10.11159/ichtd18.103">https://doi.org/10.11159/ichtd18.103</a>
- Bertagne, C., Cognata, T., Sheth, R., Dinsmore, C., & Hartl, D. (2017). Testing and Analysis of a Morphing Radiator Concept for Thermal Control of Crewed Space Vehicles. Applied Thermal Engineering, 124. https://doi.org/10.1016/j.applthermaleng.2017.06.062

- 5. Domingo-Carrillo, M. Á., Ramírez, J., Ingeniería, S., Sistemas, S., Avda, & Zugazarte. (2003). *Mechanical design and test of ROSETTA Platform Louvres*.
- Rydge B Mulford, Samuel D Salt, Lance P Hyatt, Kyle S Meaker, Vivek H Dwivedi, Matthew R Jones, Brian D Iverson (2020). Experimental Demonstration of Heat Loss and Turn-Down Ratio for a Multi-Panel, Actively Deployed Radiator. Applied Thermal Engineering, 115658. https://doi.org/10.1016/j.applthermaleng.2020.115658
- 7. Hengeveld, D., Wilson, M., Moulton, J., Taft, B., & Kwas, A. (2018). Thermal design considerations for future high-power small satellites. *Conference: 48th International Conference on Environmental Systems, July*.
- 8. Mihálcz, I. (2001). Fundamental characteristics and design method for nickel-titanium shape memory alloy. *Periodica Polytechnica, Mechanical Engineering*, *45*, 75–86.
- 9. Nagano, H., Nagasaka, Y., & Ohnishi, A. (2006). A Simple Deployable Radiator with Autonomous Thermal Control Function. *Journal of Thermophysics and Heat Transfer J THERMOPHYS HEAT TRANSFER*, 20, 856–864. https://doi.org/10.2514/1.17988
- Nagano, H., Nagasaka, Y., Ohnishi, A., Watanabe, K., Oikawa, Y., & Yamaguchi, K. (2006).
   Design and Fabrication of a Passive Deployable/Stowable Radiator. SAE Technical Papers. https://doi.org/10.4271/2006-01-2038
- 11. Nagano, H., Ohnishi, A., Higuchi, K., & Nagasaka, Y. (2009). Experimental Investigation of a Passive Deployable/Stowable Radiator. *Journal of Spacecraft and Rockets J SPACECRAFT ROCKET*, 46, 185–190. https://doi.org/10.2514/1.30170
- 12. Evans, A. (2019). Design and Testing of the CubeSat Form Factor Thermal Control Louvers. *Proceedings of the AIAA/USU Conference on Small Satellites, Technical Poster Session IV, SSC19-P4-23*. https://ntrs.nasa.gov/search.jsp?R=20190028943
- 13. Guy, W. W., and Ellis, W. E., (1963). Vacuum Chamber Heat Transmission Analysis. National Aeronautics and Space Administration, Houston, TX, Report No. NASA-TM-X-65036.
- 14. Mulford, R. B., Dwivedi, V. H., Jones, M. R., & Iverson, B. D. (2019). Control of Net Radiative Heat Transfer with a Variable-Emissivity Accordion Tessellation. *Journal of Heat Transfer*, 141(3), 1–10. <a href="https://doi.org/10.1115/1.4042442">https://doi.org/10.1115/1.4042442</a>
- 15. Vasiliev, L. L. (2005). Heat pipes in modern heat exchangers. *Applied Thermal Engineering*, 25(1), 1–19.

https://doi.org/https://doi.org/10.1016/j.applthermaleng.2003.12.004